Available online at www.sciencedirect.com
SCIENCE DIRECT®
ELSEVIER
International Journal of Solids and Structures 43 (2006) 3770–3793
INTERNATIONAL JOURNAL OF SOLIDS and STRUCTURES
www.elsevier.com/locate/ijsolstr

Analytical solutions for the time-dependent behaviour of composite beams with partial interaction

G. Ranzi [a,*], M.A. Bradford [b]

[a] *Department of Civil Engineering, The University of Sydney, Building J05, Sydney, NSW 2006, Australia*
[b] *Professor of Civil Engineering, The University of New South Wales, Sydney, NSW 2052, Australia*

Received 5 March 2005
Available online 18 April 2005

Abstract

This paper presents a generic modelling for the time-dependent analysis of composite steel–concrete beams with partial shear interaction that occurs due to the deformation of the shear connection. The time effects considered in this modelling are those that arise from shrinkage and creep deformations of the concrete slab, and these effects are modelled using algebraic representations such as those of the age-adjusted effective modulus method (AEMM) and the mean stress method (MS), which are viscoelastic models for concrete deformation that can be stated algebraically. The generic model lends itself to closed form solutions for the analysis of composite beams subjected to a generic applied loading under a variety of end conditions. In this paper, the generic model is applied for the time-dependent analysis of composite beams that are simply supported and encastré, and to a propped cantilever, that are subjected to uniformly distributed loading and shrinkage deformations. Various representations of the structural behaviour of these beams are given in closed form which can also be used to benchmark available modelling techniques, i.e. finite element and finite difference formulations, which require a spatial discretisation to be specified as well as the time discretisation to perform a time analysis.

Keywords: Composite beams; Closed form solutions; Time effects; Creep; Shrinkage; Time-dependent behaviour; Partial shear interaction

* Corresponding author. Tel.: +61 2 9351 5215; fax: +61 2 9351 3343.
E-mail address: g.ranzi@civil.usyd.edu.au (G. Ranzi).

0020-7683/$ - see front matter © 2005 Elsevier Ltd. All rights reserved.
doi:10.1016/j.ijsolstr.2005.03.032

1. Introduction

Steel–concrete composite T-beams are a popular and economical form of construction in both buildings and bridges. This paper will focus on their behaviour at service loads, which is highly affected by time effects, such as creep and shrinkage of the concrete slab.

The time-dependent analysis of composite beams with partial shear interaction (PI) requires the global behaviour of the structural system to be considered, in deference to the case of full shear interaction where a cross-sectional time analysis can be performed without investigating the global behaviour as presented by Gilbert (1988), Bradford and Gilbert (1989), and Ghali and Favre (1994). In the early 90s several researchers investigated the time-dependent behaviour of composite beams with PI; some of the first studies were published by Bradford and Gilbert (1992) and by Tarantino and Dezi (1992). Bradford and Gilbert (1992) utilised a boundary value modelling approach based on the shooting technique which they applied for the time analysis of simply supported beams using the age-adjusted effective modulus method (AEMM). Tarantino and Dezi (1992) presented an analytical model based on the finite difference method while using the step-by-step procedure to model the time-dependent behaviour of the concrete. This approach was based on the flexibility method. The following year a finite element formulation based on a 10 degrees-of-freedom finite element was proposed by Amadio and Fragiacomo (1993).

Recently, Dezi et al. (2001) investigated the interaction of shear-lag, PI and creep effects, and their approach was based on the finite difference method. Kwak and Seo (2002) proposed a numerical model which, after sub-dividing the beam into several segments, applies force equilibrium equations and strain compatibility conditions at each node assuming a piecewise linear distribution of the bending moment and of both the curvature and the strain in the bottom fibre of the concrete element due to creep deformations, while Fragiacomo et al. (2002) investigated the viscous behaviour of composite beams with normal and high performance slabs.

This paper intends to propose a formulation for the time-dependent analysis of composite beams with PI, referred to as the general method of time analysis, where the time-dependent behaviour of the concrete is modelled using algebraic methods, such as the age-adjusted effective modulus method (AEMM), the mean stress method (MS) and the effective modulus method (EM). The EM method is not considered in detail as, differently from the AEMM and MS methods, it can be simply applied using the same modelling procedures developed for the instantaneous analysis (already available in literature) while using the effective modulus for the concrete instead of its elastic one. On the other hand, the AEMM and MS methods require two analyses to fully complete the time-dependent analysis, which are an instantaneous analysis (i.e. at time t_0, where t_0 is defined as the time of first loading) and an analysis that is performed at one step in time (at the prescribed time t).

The formulation presented produces analytical results for beams with a number of support conditions, with no discretisations along the beam being introduced in the solution process. This is demonstrated for the cases of simply supported beams, propped cantilever beams and fixed ended beams subjected to a uniformly distributed load and to shrinkage deformation for which closed form solutions, which appear not to have been previously published in the open literature, have been derived. The correctness of these closed form solutions has been validated against the results of the direct stiffness method (DSM) as, similarly to the closed form solutions presented herein, it requires only one discretisation (i.e. in the time domain) to perform time analyses based on the algebraic methods instead of the two discretisations (i.e. one in the time domain and one in the spatial domain along the beam axis) required by other time-dependent modelling techniques (Ranzi, 2003). These closed form solutions can also be used to benchmark the accuracy of other modelling techniques which require a spatial discretisation (along the member length) as well as the time discretisation. This has already been briefly carried out by Ranzi et al. (2004a), where results obtained using the finite difference method and the finite element method have been considered.

2. Partial interaction analysis

The general method of time analysis presented in this paper represents a continuation in the time domain of the formulation described by Ranzi et al. (2003) for the instantaneous analysis of composite beams with PI. The modelling is based on the composite cross-section shown in Fig. 1 and, for simplicity and without any loss of generality, a single span beam is considered as shown in Fig. 2. The pattern of loading considered produces a variation of the bending moment $M(z)$ and of the axial force $N(z)$, whose variations are not necessarily known initially if the beam is statically indeterminate. For simplicity, $M(z)$ and $N(z)$ will be referred to as M_0 and N_0 at time t_0, and as M_k and N_k at time t. The subscripts '0' and 'k' are used throughout this paper to distinguish between actions and cross-sectional properties calculated at time t_0 and at time t respectively.

The composite beam considered is assumed to occupy the spatial region $V = A \cdot [0, L]$, where A represents the composite cross-section shown in Fig. 1 which is an arbitrary cross-section that is symmetric about the plane of bending, while $[0, L]$ is defined along the beam coordinate z (which is perpendicular to the cross-section at any location along the beam length, and with $z \in [0, L]$). The composite beam is comprised of a top and a bottom element, which represent the reinforced concrete slab and the steel joist respectively, and these are referred to as elements 1 and 2 respectively. The composite cross-section is thus represented as $A = A_1 \cup A_2$, where A_1 and A_2 are the cross-sections of elements 1 and 2 respectively; A_1 is further subdivided into A_c and A_r which represent the areas of the concrete component and of the reinforcement respectively, while A_2 represents the cross-section of the steel joist only and it is denoted as A_s.

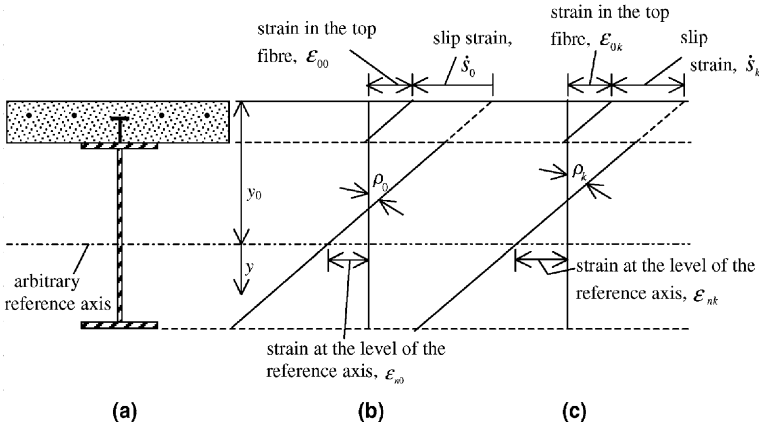

Fig. 1. Composite cross-section (a) and strain diagrams at time t_0 (b) and t (c).

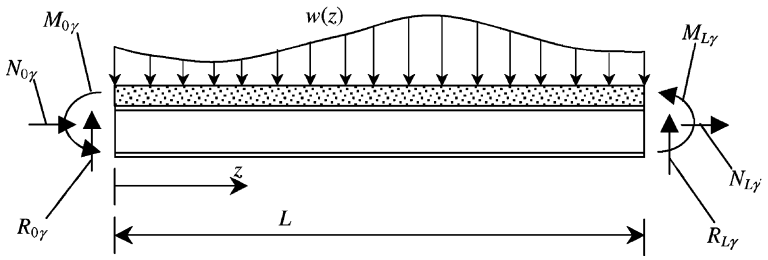

Fig. 2. General single span beam at time t_0 and at time t.

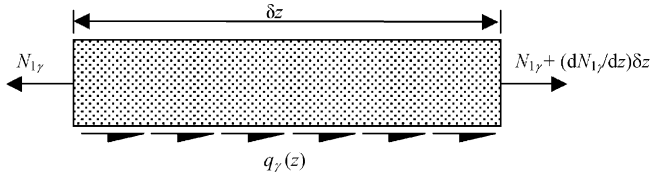

Fig. 3. Free body diagram of the top element at time t_0 and at time t.

For continuous beams, the expressions derived can be applied to each span utilising the appropriate static and/or kinematic boundary conditions and enforcing compatibility to be satisfied between adjacent spans (i.e. at support locations). Similarly, the presence of point loads would require the procedure presented to be applied between point loads and/or supports (therefore sub-dividing each span into beam segments) utilising the appropriate static and/or kinematic boundary conditions and enforcing that compatibility is satisfied between adjacent segments of the beam (i.e. at support and point load locations). For generality, the model is derived with reference to an arbitrary axis located at a distance y_0 below the top fibre of the cross-section from which the cross-sectional properties of the beam are defined. As the axial displacement is controlled at the level of the reference axis, it will be assumed, without any loss of generality, that the reference axis is located in the steel joist (i.e. bottom element) as occurs in real beams. It is also assumed that the steel joist, the steel reinforcement and the shear connection behave in a linear-elastic fashion, while the concrete behaviour is modelled by means of more complex algebraic representations.

In a similar way to Newmark's highly cited model (Newmark et al., 1951), the curvature is assumed to be the same in the top and bottom elements which leads to a condition of no vertical separation, while plane sections are assumed to remain plane with a slip discontinuity at the interface between the top and bottom elements.

The model is constructed at time t_0 and at time t based on an unknown strain diagram, which requires three parameters to be fully defined, which are the strain in the top fibre of the cross-section $\tilde{\varepsilon}_{0\gamma}$, the curvature ρ_γ and the slip strain $\frac{ds_\gamma}{dz}$ (where $\gamma = 0, k$ at time t_0 and t respectively). For simplicity $\frac{ds_\gamma}{dz}$ will be denoted as $\dot{s}_\gamma$. The three equations utilised to solve the problem are those for horizontal equilibrium at the composite cross-section, rotational equilibrium at the composite cross-section and horizontal equilibrium of a free body diagram of the top element as shown in Fig. 3.

In the following the material properties considered in the modelling are firstly defined. The formulation of the modelling technique applied to both instantaneous and time analyses is then presented, and closed form solutions are derived for the cases of simply supported beams, propped cantilever beams and fixed ended beams subjected to a uniformly distributed load and to shrinkage deformation. These are then validated against the results obtained using the direct stiffness method (DSM).

3. Material properties

The generic composite cross-section considered in this paper is formed by a concrete component, reinforcing bars, a steel joist and a shear connection as shown in Fig. 1. The steel reinforcement and the steel joist are assumed to behave in a linear-elastic fashion at times t_0 and t as

$$\sigma_{r\gamma} = E_r \varepsilon_{r\gamma} = E_r \lfloor \tilde{\varepsilon}_{0\gamma} + (y + y_0)\rho_\gamma \rfloor \tag{1a}$$

$$\sigma_{s\gamma} = E_s \varepsilon_{s\gamma} = E_s \lfloor \tilde{\varepsilon}_{0\gamma} + (y + y_0)\rho_\gamma + \dot{s}_\gamma \rfloor \tag{1b}$$

where y is the vertical coordinate from the reference axis, $\sigma_{r\gamma}$ and $\varepsilon_{r\gamma}$ are the generic stress and strain in the steel reinforcement, $\sigma_{s\gamma}$ and $\varepsilon_{s\gamma}$ are the generic stress and strain in the steel joist, and E_s and E_r are the elastic

moduli of the steel joist and reinforcement respectively. The shear connection is also assumed to behave in a linear-elastic fashion so that

$$q_\gamma = k s_\gamma \tag{2}$$

where q_γ is the shear flow per unit length (shear flow force), k is the shear connection stiffness (force per length^2), and s_γ is the slip.

The behaviour of the concrete is assumed to be time-dependent, and it is modelled using the AEMM and MS methods and, therefore, incorporating all the limitations of these algebraic formulations (CEB, 1984; Bažant, 1972; Trost, 1967). These have been recommended by Dezi et al. (1996, 1998) for the analysis of composite beams based on a parametric study carried out benchmarking the results obtained using different algebraic representations against those using the step-by-step method. In particular, they recommended the use of the AEMM method to model the time-dependent behaviour of the concrete when the structural system is subjected to external loads, while using the MS method to consider shrinkage effects. It is also assumed that the time-dependent behaviour of the concrete is identical in both compression and tension, as recommended by Gilbert (1988) and Bažant and Oh (1984) for stress levels in compression less than about one half of the compressive strength of the concrete, and for tensile stresses less than about one half of the tensile strength of the concrete; and so the results obtained using the proposed approach are assumed to be acceptable from a qualitative and quantitative viewpoint when the calculated stresses remain in this stress range. Nevertheless, when the calculated stresses are outside this range the results might still be meaningful from a qualitative viewpoint, for example in comparing the effects of different cross-sectional properties. The time-dependent behaviour of the concrete in both compression and tension is then defined at time t_0 and at time t as (CEB, 1984; Bažant, 1972)

$$\sigma_{c0} = E_c \varepsilon_{c0} = E_c[\tilde{\varepsilon}_{00} + (y + y_0)\rho_0] \tag{3a}$$

$$\sigma_{ck} = E_e(\varepsilon_{ck} - \varepsilon_{sh}) + \tilde{\varphi}\sigma_{c0} = E_e[\tilde{\varepsilon}_{0k} + (y + y_0)\rho_k] + \tilde{\varphi}\sigma_{c0} - E_e\varepsilon_{sh} \tag{3b}$$

and

$$\tilde{\varphi} = \frac{\phi_0(t,t_0)[\chi(t,t_0) - 1]}{1 + \chi(t,t_0)\phi_0(t,t_0)}; \quad E_e = \frac{E_{c0}}{1 + \chi(t,t_0)\phi_0(t,t_0)} \tag{4a, b}$$

$$\chi(t,t_0) = \begin{cases} \frac{E_{c0}}{E_{c0} - r(t,t_0)} - \frac{1}{\phi_0(t,t_0)} & \text{AEMM} \\ 0.5 + 0.5\frac{E_{c0}}{\phi_0(t,t_0)}\left(\frac{1}{E_{ck}} - \frac{1}{E_{c0}}\right) & \text{MS} \end{cases} \tag{4c}$$

where $\sigma_{c\gamma}$ and $\varepsilon_{c\gamma}$ are the stress and strain in the concrete component, E_{c0} and E_{ck} are the elastic moduli of the concrete at time t_0 and at time t respectively, E_e is the age-adjusted effective modulus, ε_{sh} is the shrinkage strain at time t, $\chi(t,t_0)$ is the aging coefficient, $\phi_0(t,t_0)$ is the creep coefficient defined as the ratio between the creep strain at time t and the initial strain at time t_0, and $r(t,t_0)$ is the relaxation function. The representation of the second of Eq. (4c) allows the MS method to be considered as a particular case of the AEMM method. It is worth noting that Eq. (4c) becomes exact if the stress and strain histories are linear combinations of histories obtained in the creep and relaxation problems (Bažant, 1972); this is not the case for the concrete slab in a steel–concrete composite beam (Trost, 1967). Also, unlike the MS method, the AEMM method requires the knowledge of the relaxation function $r(t,t_0)$.

4. Instantaneous analysis at time t_0

The modelling procedure proposed for the instantaneous analysis of composite beams is described briefly in this section, with a detailed derivation being given by Ranzi et al. (2003). For ease of reference all notation is defined in Appendix A.

4.1. Horizontal and rotational equilibrium

Horizontal and rotational equilibrium are established by equating the internal actions (i.e. N_{i0} and M_{i0}) to the external ones (i.e. N_0 and M_0) as

$$N_{i0} = N_{10} + N_{20} = N_0; \quad M_{i0} = M_0 \tag{5a, b}$$

where the internal actions are determined as

$$M_{i0} = \int_A y\sigma_0 \, \mathrm{d}A = B\widetilde{E}_0\tilde{\varepsilon}_{00} + I\widetilde{E}_0\rho_0 + y_0 B\widetilde{E}_0\rho_0 + B\widetilde{E}_{20}\dot{s}_0 \tag{6a}$$

$$N_{10} = \int_{A_1} \sigma_0 \, \mathrm{d}A = A\widetilde{E}_{10}\tilde{\varepsilon}_{00} + B\widetilde{E}_{10}\rho_0 + y_0 A\widetilde{E}_{10}\rho_0 \tag{6b}$$

$$N_{20} = \int_{A_2} \sigma_0 \, \mathrm{d}A = A\widetilde{E}_{20}\tilde{\varepsilon}_{00} + B\widetilde{E}_{20}\rho_0 + y_0 A\widetilde{E}_{20}\rho_0 + A\widetilde{E}_{20}\dot{s}_0 \tag{6c}$$

and N_{i0} and M_{i0} are the internal axial force and moment resisted by the composite cross-section at time t_0, N_{10} and N_{20} are the internal axial forces resisted by the top and bottom elements respectively (i.e. elements 1 and 2) at time t_0, σ_0 is the generic stress in the composite cross-section at time t_0, $\tilde{\varepsilon}_{00}$, ρ_0 and $\dot{s}_0$ are the strain in the top fibre of the composite cross-section, the curvature and the slip strain respectively at time t_0, while the cross-sectional properties are defined in Appendix A.

Based on Eq. (5a) the strain in the top fibre of the cross-section $\tilde{\varepsilon}_{00}$ can be expressed as a function of the other two unknowns, which are the curvature ρ_0 and the slip strain $\dot{s}_0$, as

$$\tilde{\varepsilon}_{00} = -\frac{B\widetilde{E}_0 + y_0 A\widetilde{E}_0}{A\widetilde{E}_0}\rho_0 - \frac{A\widetilde{E}_{20}}{A\widetilde{E}_0}\dot{s}_0 + \frac{1}{A\widetilde{E}_0}N_0 \tag{7}$$

Substituting Eq. (7) into Eq. (5b), the curvature ρ_0 can be expressed as a function of the unknown slip strain $\dot{s}_0$ as

$$\rho_0 = \frac{1}{A\widetilde{E}_0 I\widetilde{E}_0 - B\widetilde{E}_0^2}\left[A\widetilde{E}_0 M_0 - B\widetilde{E}_0 N_0 + \left(B\widetilde{E}_0 A\widetilde{E}_{20} - B\widetilde{E}_{20}A\widetilde{E}_0\right)\dot{s}_0\right] \tag{8}$$

The axial force resisted by element 1, which will be required in the following, is determined substituting Eqs. (7) and (8) into Eq. (6b) as

$$N_{10} = q_{10}M_0 + q_{20}N_0 + q_{30}\dot{s}_0 \tag{9}$$

where q_{i0} $(i = 1, 2, 3)$ are defined in Appendix A.

4.2. Horizontal equilibrium of a free body diagram of the top element

The slip strain is then obtained by enforcing horizontal equilibrium of a free body diagram of the top element at time t_0 as shown in Fig. 3, which can be written as:

$$\frac{\mathrm{d}N_{10}}{\mathrm{d}z} + q_0 = \frac{\mathrm{d}N_{10}}{\mathrm{d}z} + ks_0 = 0 \tag{10}$$

where N_{10} is the axial force resisted by the top element at time t_0. Eq. (10) represents the governing differential equation of the PI problem at time t_0. Substituting Eq. (9) into Eq. (10) this can be re-arranged in the following compact form as

$$\tilde{\alpha}_0 \frac{d^2 s_0}{dz^2} - k s_0 = \alpha_0 \frac{dM_0}{dz} + \alpha_{10} \frac{dN_0}{dz} \tag{11}$$

Eq. (11) can be solved for the slip and slip strain as the sum of a general solution corresponding to the homogeneous differential equation $s_{0.H}$ and a particular solution $s_{0.P}$ as

$$s_0 = s_{0.H} + s_{0.P} = C_{10} e^{\mu_0 z} + C_{20} e^{-\mu_0 z} + s_{0.P} \tag{12a}$$

$$\dot{s}_0 = \dot{s}_{0.H} + \dot{s}_{0.P} = \mu_0 C_{10} e^{\mu_0 z} - \mu_0 C_{20} e^{-\mu_0 z} + \dot{s}_{0.P} \tag{12b}$$

in which C_{i0} $(i = 1, 2)$ are constants of integration obtained by enforcing the static and/or kinematic boundary conditions for the beam analysed, and the actual expression for $s_{0.P}$ depends on the applied loading conditions. Once the slip and the slip strain are obtained from Eq. (12), the other variables defining the strain diagram can be determined from Eqs. (7) and (8). At this point is then possible to obtain the expressions of all other variables describing the structural behaviour of the beam at time t_0.

4.3. Actions resisted by the concrete component at time t_0

The stress state at time t is determined as a function of the stress state at time t_0 as shown in Eq. (3b). For the purpose of the present model, the stress state at time t_0 is considered in the formulation in terms of the moment M_{c0} and axial force N_{c0} resisted by the concrete component at time t_0, which are calculated as

$$M_{c0} = \int_{A_c} y \sigma_{c0} \, dA = \phi_{c10} \tilde{\varepsilon}_{00} + \phi_{c20} \rho_0 \tag{13a}$$

$$N_{c0} = \int_{A_c} \sigma_{c0} \, dA = \phi_{c30} \tilde{\varepsilon}_{00} + \phi_{c40} \rho_0 \tag{13b}$$

where A_c is the area of the concrete component, and $\tilde{\varepsilon}_{00}$ and ρ_0 are the strain in the top fibre of the composite cross-section and the curvature along the beam determined from the instantaneous analysis.

5. Time analysis

5.1. General

The formulation of the general method of analysis dealing with the time analysis is presented in this section, while its detailed derivation has been outlined by Ranzi (2003). For ease of reference all notations are defined in Appendix A.

5.2. Horizontal and rotational equilibrium

The internal actions resisted by the composite cross-section at time t are

$$N_{1k} = \int_{A_1} \sigma_k \, dA = A \widetilde{E}_{1k} \tilde{\varepsilon}_{0k} + B \widetilde{E}_{1k} \rho_k + y_0 A \widetilde{E}_{1k} \rho_k + \tilde{\varphi} N_{c0} - A_c E_e \varepsilon_{sh} \tag{14a}$$

$$N_{2k} = \int_{A_2} \sigma_k \, dA = A \widetilde{E}_{2k} \tilde{\varepsilon}_{0k} + B \widetilde{E}_{2k} \rho_k + y_0 A \widetilde{E}_{2k} \rho_k + A \widetilde{E}_{2k} \dot{s}_k \tag{14b}$$

$$M_{ik} = \int_A y\sigma_k \, \mathrm{d}A = B\widetilde{E}_k\tilde{\varepsilon}_{0k} + I\widetilde{E}_k\rho_k + y_0 B\widetilde{E}_k\rho_k - B_c E_e \varepsilon_{sh} + M_{c0}\tilde{\varphi} + B\widetilde{E}_{2k}\dot{s}_k \tag{14c}$$

where σ_k is the generic stress calculated at time t at the composite cross-section. Horizontal and rotational equilibrium at the composite cross-section is then enforced as

$$N_{ik} = N_{1k} + N_{2k} = N_k; \quad M_{ik} = M_k \tag{15a, b}$$

It is worth noting that the expressions for the internal axial force and for the internal moment are a function not only of the strain state at time t due to the applied loading, but also of the stress state occurred at time t_0 and of the shrinkage deformation at time t, as depicted in Eqs. (14a) and (14c).

The expression for the strain in the top fibre of the cross-section $\tilde{\varepsilon}_{0k}$ can be obtained from Eq. (15a) as

$$\tilde{\varepsilon}_{0k} = -\frac{B\widetilde{E}_k + y_0 A\widetilde{E}_k}{A\widetilde{E}_k}\rho_k - \frac{\tilde{\varphi}N_{c0}}{A\widetilde{E}_k} + \frac{A_c E_e}{A\widetilde{E}_k}\varepsilon_{sh} - \frac{A\widetilde{E}_{2k}}{A\widetilde{E}_k}\dot{s}_k + \frac{1}{A\widetilde{E}_k}N_k \tag{16}$$

while the curvature ρ_k can be obtained substituting Eq. (16) into Eq. (15b) as

$$\rho_k = \frac{1}{A\widetilde{E}_k I\widetilde{E}_k - B\widetilde{E}_k^2}\left[A\widetilde{E}_k M_k - B\widetilde{E}_k N_k - A\widetilde{E}_k M_{c0}\tilde{\varphi} + B\widetilde{E}_k N_{c0}\tilde{\varphi} + \left(B\widetilde{E}_k A\widetilde{E}_{2k} - B\widetilde{E}_{2k}A\widetilde{E}_k\right)\dot{s}_k + \left(A\widetilde{E}_k B_c E_e - B\widetilde{E}_k A_c E_e\right)\varepsilon_{sh}\right] \tag{17}$$

Substituting Eqs. (16) and (17) into Eq. (14a) yields the axial force resisted by the top element at time t as

$$N_{1k} = q_{1k}M_k + q_{2k}N_k + q_{3k}\dot{s} - q_{1k}M_{c0}\tilde{\varphi} - q_{4k}N_{c0}\tilde{\varphi} + Sh_{4k}\varepsilon_{sh} \tag{18}$$

5.3. Horizontal equilibrium of a free body diagram of the top element

Based on Eq. (15) the PI problem can be expressed as a function of only one unknown (i.e. the slip strain). The additional equation utilised in this approach to derive the expression for the slip strain is the one of horizontal equilibrium at time t of a free body diagram of the top element as shown in Fig. 3. This can be stated as

$$\frac{\mathrm{d}N_{1k}}{\mathrm{d}z} + q_k = \frac{\mathrm{d}N_{1k}}{\mathrm{d}z} + ks_k = 0 \tag{19}$$

where N_{1k} is the axial force resisted by the top element at time t, q_k is the shear flow force at time t, and s_k is the slip along the beam at time t.

Eq. (19) represents the governing differential equation of the PI problem and can be re-arranged based on Eq. (18) in the following compact form as

$$\tilde{\alpha}_k\frac{\mathrm{d}^2 s_k}{\mathrm{d}z^2} - ks_k = \alpha_k\frac{\mathrm{d}M_k}{\mathrm{d}z} - \alpha_k\tilde{\varphi}\frac{\mathrm{d}M_{c0}}{\mathrm{d}z} + \alpha_{1k}\frac{\mathrm{d}N_k}{\mathrm{d}z} - \alpha_{2k}\tilde{\varphi}\frac{\mathrm{d}N_{c0}}{\mathrm{d}z} \tag{20}$$

The general solution of the governing nonhomogeneous linear differential equation for the slip can be produced routinely again as the sum of a general solution corresponding to the homogeneous differential equation $s_{k.H}$ and a particular solution $s_{k\cdot P}$ as

$$s_k = s_{k.H} + s_{k.P} = C_{1k}\mathrm{e}^{\mu_k z} + C_{2k}\mathrm{e}^{-\mu_k z} + s_{k.P} \tag{21a}$$

$$\dot{s}_k = \dot{s}_{k.H} + \dot{s}_{k.P} = \mu_k C_{1k}\mathrm{e}^{\mu_k z} - \mu_k C_{2k}\mathrm{e}^{-\mu_k z} + \dot{s}_{k.P} \tag{21b}$$

in which C_{ik} $(i = 1, 2)$ are constants of integration derived by enforcing the static and/or kinematic boundary conditions for the beam analysed, and the expression for $s_{k\cdot P}$ depends on the applied loading conditions. Once the slip and slip strain are determined from Eq. (21), the expressions for the other unknowns (i.e. the curvature and the strain in the top fibre of the cross-section) can be determined from Eqs. (16) and (17).

6. Structural behaviour at times t_0 and t

Based on the formulation presented in the previous sections for the instantaneous analysis and for the time analysis, the structural behaviour of a composite beam can be fully defined.

Once the slip and slip strain are obtained from Eqs. (12) and (21) for the analyses at time t_0 and at time t respectively, the expressions for the other two unknowns utilised in the formulation to define the strain diagram (i.e. the curvature and the strain in the top fibre of the cross-section) are determined based on Eqs. (7), (8), (16) and (17), which can be re-arranged in a more compact form as outlined below. All other variables describing the structural behaviour can then be derived.

The following expressions are derived for the behaviour at both time t_0 and at time t owing to their similarities, while the identities $\tilde{\delta}_0 \equiv 0$, $\tilde{\delta}_k \equiv 1$ are used, and obviously $\varepsilon_{sh} = 0$ for the instantaneous analysis $(\gamma = 0)$. Hence

$$\tilde{\varepsilon}_{0\gamma} = b_{1\gamma} M_\gamma + b_{2\gamma} N_\gamma + b_{3\gamma} \dot{s}_\gamma + (-b_{1k} M_{c0} \tilde{\varphi} - b_{2k} N_{c0} \tilde{\varphi}) \tilde{\delta}_\gamma + Sh_{1k} \varepsilon_{sh} \tag{22}$$

$$\rho_\gamma = r_{1\gamma} M_\gamma + r_{2\gamma} N_\gamma + r_{3\gamma} \dot{s}_\gamma + (-r_{1k} M_{c0} \tilde{\varphi} - r_{2k} N_{c0} \tilde{\varphi}) \tilde{\delta}_\gamma + Sh_{2k} \varepsilon_{sh} \tag{23}$$

where M_{c0} and N_{c0} are calculated based on Eq. (13) and for ease of reference all notation is defined in Appendix A.

The expressions for the rotation and deflection can then be obtained by integrating the curvature about the coordinate along the beam length z. Hence,

$$\theta_\gamma = r_{1\gamma} \int M_\gamma \, dz + r_{2\gamma} \int N_\gamma \, dz + r_{3\gamma} \int \dot{s}_\gamma \, dz + \left(-r_{1k} \tilde{\varphi} \int M_{c0} \, dz - r_{2k} \tilde{\varphi} \int N_{c0} \, dz + Sh_{2k} \varepsilon_{sh} z \right) \tilde{\delta}_\gamma + \widehat{C}_{1\gamma} \tag{24}$$

$$\begin{aligned} v_\gamma = {} & r_{1\gamma} \int \int M_\gamma \, dz \, dz + r_{2\gamma} \int \int N_\gamma \, dz \, dz + r_{3\gamma} \int \int \dot{s}_\gamma \, dz \, dz + \widehat{C}_{1\gamma} z + \widehat{C}_{2\gamma} \\ & + \left(-r_{1k} \tilde{\varphi} \int \int M_{c0} \, dz \, dz - r_{2k} \tilde{\varphi} \int \int N_{c0} \, dz \, dz \right) \tilde{\delta}_\gamma + \frac{Sh_{2k} \varepsilon_{sh}}{2} z^2 \end{aligned} \tag{25}$$

and the strain at the level of the reference axis is determined as

$$\tilde{\varepsilon}_{b\gamma} = l_{1\gamma} M_\gamma + l_{2\gamma} N_\gamma + l_{3\gamma} \dot{s}_\gamma + (-l_{1k} M_{c0} \tilde{\varphi} - l_{2k} N_{c0} \tilde{\varphi}) \tilde{\delta}_\gamma + Sh_{3k} \varepsilon_{sh} \tag{26}$$

By integrating $\tilde{\varepsilon}_{b\gamma}$ over the beam length, the axial displacement at the level of the reference axis $u_{b\gamma}$ can be determined as

$$u_{b\gamma} = l_{1\gamma} \int M_\gamma \, dz + l_{2\gamma} \int N_\gamma \, dz + l_{3\gamma} \int \dot{s}_\gamma \, dz + \left(-l_{1k} \tilde{\varphi} \int M_{c0} \, dz - l_{2k} \tilde{\varphi} \int N_{c0} \, dz \right) \tilde{\delta}_\gamma + Sh_{3k} \varepsilon_{sh} z + C_{u\gamma} \tag{27}$$

7. Structural application

Eqs. (12) and (21) to (27) form the basis for investigating the instantaneous and the time-dependent behaviour of composite beams with PI using a variety of end conditions. The use of these equations is illustrated in this section for the instantaneous and time analyses of a generic beam subjected to the loading condition illustrated in Fig. 4; this implies, without any loss of generality, that the expressions for M_γ and N_γ considered are of the second and zero order in z (where z is the coordinate along the beam), so that from elementary statics

$$M_\gamma = -M_{0\gamma} + R_{0\gamma} z - \frac{wz^2}{2}; \quad N_\gamma = -N_{0\gamma} \tag{28a, b}$$

where $M_{0\gamma}$, $R_{0\gamma}$ and $N_{0\gamma}$ are defined in Fig. 4. Expressions for M_γ and N_γ of higher orders could be easily considered, but the derivation would need to be modified accordingly.

7.1. Modelling at time t_0 and at time t

The general method of time analysis for composite beams with PI subjected to the loading conditions defined in Eq. (28) is outlined in this section. A compact formulation is adopted for this purpose which has the advantage of highlighting the relevant and unknown terms, which are the coordinate along the beam length z, the unknown reactions at the left support ($z = 0$) $N_{0\gamma}$, $R_{0\gamma}$, $M_{0\gamma}$ (as the reactions at the right support ($z = L$) $N_{L\gamma}$, $R_{L\gamma}$, $M_{L\gamma}$ can be determined from elementary statics) and the constants of integration for the slip expression C_{1k} and C_{2k} which can be determined once the static and/or kinematic boundary conditions of the beam are enforced. This method is then applied to the cases of a simply supported beam, of a fixed ended beam and of a propped cantilever beam subjected to a uniformly distributed load and to shrinkage deformation, and with the slab undergoing creep.

Based on the loading conditions considered, the expressions for the moment M_{c0} and axial force N_{c0} resisted by the concrete component required by the analysis at time t can be re-arranged for clarity and to avoid lengthy expressions in the following compact and generic form based on Eq. (13) as

$$M_{c0} = a_{10} + a_{20} z + a_{30} z^2 + a_{40} e^{\mu_0 z} + a_{50} e^{-\mu_0 z} \tag{29a}$$

$$N_{c0} = a_{110} + a_{120} z + a_{130} z^2 + a_{140} e^{\mu_0 z} + a_{150} e^{-\mu_0 z} \tag{29b}$$

The slip and slip strain can then be expressed as

$$s_\gamma = C_{1\gamma} e^{\mu_\gamma z} + C_{2\gamma} e^{-\mu_\gamma z} - \frac{\alpha_\gamma}{k}(R_{0\gamma} - wz) + \psi_{1\gamma} + \psi_{2\gamma} z + \psi_{3\gamma} e^{\mu_0 z} + \psi_{4\gamma} e^{-\mu_0 z} \tag{30}$$

$$\dot{s}_\gamma = \mu_\gamma C_{1\gamma} e^{\mu_\gamma z} - \mu_\gamma C_{2\gamma} e^{-\mu_\gamma z} + \frac{\alpha_\gamma w}{k} + \psi_{2\gamma} + \mu_0 \psi_{3\gamma} e^{\mu_0 z} - \mu_0 \psi_{4\gamma} e^{-\mu_0 z} \tag{31}$$

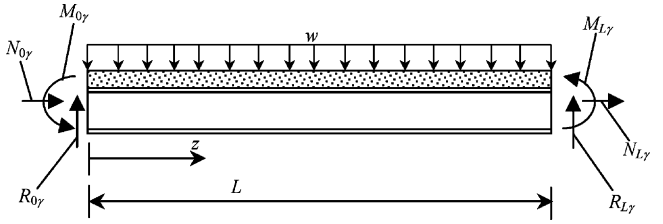

Fig. 4. General single span beam at time t_0 and at time t.

The strain in the top fibre of the cross-section, the curvature, the rotation and the deflection along the beam can be expressed as

$$\tilde{\varepsilon}_{0\gamma} = \left\{-b_{1\gamma}M_{0\gamma} - b_{2\gamma}N_{0\gamma} + \beta_{1\gamma}\right\} + \left\{b_{1\gamma}R_{0\gamma} + \beta_{2\gamma}\right\}z + \beta_{3\gamma}z^2 + b_{3\gamma}\mu_\gamma C_{1\gamma}e^{\mu_\gamma z} - b_{3\gamma}\mu_\gamma C_{2\gamma}e^{-\mu_\gamma z} + \beta_{4\gamma}e^{\mu_0 z} + \beta_{5\gamma}e^{-\mu_0 z} \tag{32}$$

$$\rho_\gamma = \left\{-r_{1\gamma}M_{0\gamma} - r_{2\gamma}N_{0\gamma} + \xi_{1\gamma}\right\} + \left\{r_{1\gamma}R_{0\gamma} + \xi_{2\gamma}\right\}z + \xi_{3\gamma}z^2 + r_{3\gamma}\mu_\gamma C_{1\gamma}e^{\mu_\gamma z} - r_{3\gamma}\mu_\gamma C_{2\gamma}e^{-\mu_\gamma z} + \xi_{4\gamma}e^{\mu_0 z} + \xi_{5\gamma}e^{-\mu_0 z} \tag{33}$$

$$\theta_\gamma = \left\{-r_{1\gamma}M_{0\gamma} - r_{2\gamma}N_{0\gamma} + \xi_{1\gamma}\right\}z + \left\{\frac{r_{1\gamma}R_{0\gamma}}{2} + \frac{\xi_{2\gamma}}{2}\right\}z^2 + \frac{\xi_{3\gamma}}{3}z^3 + r_{3\gamma}C_{1\gamma}e^{\mu_\gamma z} + r_{3\gamma}C_{2\gamma}e^{-\mu_\gamma z} + \frac{\xi_{4\gamma}}{\mu_0}e^{\mu_0 z} - \frac{\xi_{5\gamma}}{\mu_0}e^{-\mu_0 z} + \widehat{C}_{1\gamma} \tag{34}$$

$$v_\gamma = \left\{-\frac{r_{1\gamma}M_{0\gamma}}{2} - \frac{r_{2\gamma}N_{0\gamma}}{2} + \frac{\xi_{1\gamma}}{2}\right\}z^2 + \left\{\frac{r_{1\gamma}R_{0\gamma}}{6} + \frac{\xi_{2\gamma}}{6}\right\}z^3 + \frac{\xi_{3\gamma}}{12}z^4 + \frac{r_{3\gamma}C_{1\gamma}e^{\mu_\gamma z}}{\mu_\gamma} - \frac{r_{3\gamma}C_{2\gamma}e^{-\mu_\gamma z}}{\mu_\gamma} + \frac{\xi_{4\gamma}}{\mu_0^2}e^{\mu_0 z} + \frac{\xi_{5\gamma}}{\mu_0^2}e^{-\mu_0 z} + \widehat{C}_{1\gamma}z + \widehat{C}_{2\gamma} \tag{35}$$

The strain and the axial displacement at the level of the reference axis are

$$\tilde{\varepsilon}_{b\gamma} = \left\{-l_{1\gamma}M_{0\gamma} - l_{2\gamma}N_{0\gamma} + \eta_{1\gamma}\right\} + \left\{l_{1\gamma}R_0 + \eta_{2\gamma}\right\}z + \eta_{3\gamma}z^2 + l_{3\gamma}\mu_\gamma C_{1\gamma}e^{\mu_\gamma z} - l_{3\gamma}\mu_\gamma C_{2\gamma}e^{-\mu_\gamma z} + \eta_{4\gamma}e^{\mu_0 z} + \eta_{5\gamma}e^{-\mu_0 z} \tag{36}$$

$$u_{b\gamma} = \left\{-l_{1\gamma}M_{0\gamma} - l_{2\gamma}N_{0\gamma} + \eta_{1\gamma}\right\}z + \left\{\frac{l_{1\gamma}R_{0\gamma}}{2} + \frac{\eta_{2\gamma}}{2}\right\}z^2 + \frac{\eta_{3\gamma}}{3}z^3 + l_{3\gamma}C_{1\gamma}e^{\mu_\gamma z} + l_{3\gamma}C_{2\gamma}e^{-\mu_\gamma z} + \frac{\eta_{4\gamma}e^{\mu_0 z}}{\mu_0} - \frac{\eta_{5\gamma}e^{-\mu_0 z}}{\mu_0} + C_{u\gamma} \tag{37}$$

The constants of integration $\widehat{C}_{1\gamma}$, $\widehat{C}_{2\gamma}$ and $C_{u\gamma}$ may then be determined, by applying the kinematic boundary conditions that $v_\gamma(z=0)=0$, $v_\gamma(z=L)=0$ and $u_{b\gamma}(z=0)=0$, as

$$\widehat{C}_{1\gamma} = \frac{L}{2}(r_{1\gamma}M_{0\gamma} + r_{2\gamma}N_{0\gamma} - \xi_{1\gamma}) - \frac{L^2}{6}(r_{1\gamma}R_{0\gamma} + \xi_{2\gamma}) - \frac{\xi_{3\gamma}L^3}{12} - \overline{C}_\gamma \tag{38}$$

$$\widehat{C}_{2\gamma} = \frac{r_{3\gamma}}{\mu_\gamma}(C_{2\gamma} - C_{1\gamma}) - \frac{\xi_{4\gamma} + \xi_{5\gamma}}{\mu_0^2} \tag{39}$$

$$C_{u\gamma} = -l_{3\gamma}(C_{1\gamma} + C_{2\gamma}) - \frac{\eta_{4\gamma} - \eta_{5\gamma}}{\mu_0} \tag{40}$$

where

$$\overline{C}_\gamma = \frac{r_{3\gamma}}{\mu_\gamma L}\left[C_{1\gamma}\left(e^{\mu_\gamma L} - 1\right) - C_{2\gamma}\left(e^{-\mu_\gamma L} - 1\right)\right] + \frac{1}{\mu_0^2 L}\left[\xi_{4\gamma}\left(e^{\mu_0 L} - 1\right) + \xi_{5\gamma}\left(e^{-\mu_0 L} - 1\right)\right] \tag{41}$$

In this form, the constants of integration $C_{1\gamma}$ and $C_{2\gamma}$ can be prescribed by imposing the static and/or kinematic boundary conditions for the relevant beam type, as illustrated in the following sub-sections for a simply supported beam, for a beam encastré at both ends and for a propped cantilever; the correctness of the

closed form solutions presented for these structural systems is validated against the results obtained by means of the direct stiffness method described by Ranzi (2003), which, similarly to the closed form solutions derived herein, requires only one discretisation (i.e. in the time domain) to perform time analyses based on the algebraic representation of the concrete rheology. For this purpose, the time-dependent behaviour of the concrete has been modelled by means of the AEMM method when subjected to external loads (i.e. uniformly distributed loading) and by means of the MS method to account for shrinkage effects as recommended by Dezi et al. (1996, 1998). For the comparisons, the composite cross-sectional and material properties utilised are summarised in Tables 1 and 2, while the results have been plotted for various levels of the dimensionless stiffness parameter $\mu_k L$ (which is calculated based on the cross-sectional and material properties at time t); this term $\mu_0 L$ (when calculated at time t_0) has been shown by Ranzi et al. (2004b) to be equivalent to the dimensionless stiffness term αL identified by Girhammar and Pan (1993).

7.2. Simply supported beam subject to a uniformly distributed load and to shrinkage deformation

The reactions at time t for the simply supported beam shown in Fig. 5 are determined from elementary statics as

$$R_{0k} = R_{Lk} = \frac{wL}{2}; \quad M_{0k} = M_{Lk} = 0; \quad N_{0k} = N_{Lk} = 0 \tag{42a, b, c}$$

The expressions for the slip and slip strain are then determined using Eqs. (30) and (31) where the constants of integration C_{1k} and C_{2k} are calculated applying the boundary conditions that $\dot{s}(z=0) = -\tilde{\varepsilon}_{\mathrm{sh}}$ and $\dot{s}(z=L) = -\tilde{\varepsilon}_{\mathrm{sh}}$.

$$s_k = \tilde{\bar{e}}_k(z) + \frac{w}{k}\left[\tilde{\lambda}_2 \tilde{\bar{e}}_0(z) - \left(\frac{L}{2} - z\right)\tilde{\lambda}_{1\alpha}\right] \tag{43}$$

$$\dot{s}_k = v_k \tilde{e}_k(z) + \frac{w}{k}\left[\tilde{\lambda}_2 \mu_0 \tilde{e}_0(z) + \tilde{\lambda}_{1\alpha}\right] \tag{44}$$

The strain in the top fibre of the cross-section, the curvature, the rotation and the deflection along the beam can be determined as

$$\tilde{\varepsilon}_{0k} = \frac{wz}{2}(L-z)\tilde{\lambda}_{1b} + b_{3k}\mu_k \tilde{e}_k(z) + \frac{w}{k}\left[\mu_0 \tilde{\lambda}_{3b}\tilde{e}_0(z) + \tilde{\lambda}_{4b}\right] + Sh_{1k}\varepsilon_{\mathrm{sh}} \tag{45}$$

$$\rho_k = \frac{wz}{2}(L-z)\tilde{\lambda}_{1r} + r_{3k}\mu_k \tilde{e}_k(z) + \frac{w}{k}\left[\mu_0 \tilde{\lambda}_{3r}\tilde{e}_0(z) + \tilde{\lambda}_{4r}\right] + Sh_{2k}\varepsilon_{\mathrm{sh}} \tag{46}$$

$$\theta_k = \frac{wz^2}{12}(3L-2z)\tilde{\lambda}_{1r} + r_{3k}\tilde{\bar{e}}_k(z) + \frac{w}{k}\left[\tilde{\lambda}_{3r}\tilde{\bar{e}}_0(z) + \tilde{\lambda}_{4r}z\right] + Sh_{2k}\varepsilon_{\mathrm{sh}}z + \widehat{C}_{1k} \tag{47}$$

Table 1
Composite cross-sectional properties: steel joist and reinforcement

Steel joist		Reinforcement	
Section	1200WB455 (Australian section)	A_r	8050 mm^2
		Location	At mid-height of slab
Flange	500 mm × 40 mm	E_r	210,000 MPa
Web	1120 mm × 16 mm		
E_s	210,000 MPa		

Table 2
Composite cross-sectional properties: concrete component

Concrete component		
B	3500 mm	Width of slab
D	230 mm	Depth of slab
f'_c	32 MPa	Cylinder compressive strength
E_c	27,783 MPa	Elastic modulus of the concrete at 4 days
	34,129 MPa	Elastic modulus of the concrete at 28 days
	38,418 MPa	Elastic modulus of the concrete at 10,000 days
s	0.25	Coefficient which depends on the type of cement ($s = 0.25$ for normal and rapid hardening cements N and R)
t_0	28 days	Age of concrete at loading (days)
t_f	10,000 days	Age of concrete (days) at the time considered
RH	70%	Relative humidity of ambient environment (%)
H	231.32	Notational size of member (mm)
t_s	4 days	Age of concrete (days) at the beginning of shrinkage
β_{sc}	5	Coefficient which depends on the type of cement ($\beta_{sc} = 5$ for normal and rapid hardening cements N and R)
Creep and shrinkage coefficients		
ϕ_0	1.898460[a]	Creep coefficient based on $t_0 = 28$ days and $t_f = 10{,}000$ days
	2.229048[b]	Creep coefficient based on $t_0 = t_s = 4$ days and $t_f = 10{,}000$ days
χ	0.837416[a]	Aging coefficient based on $t_0 = 28$ days and $t_f = 10{,}000$ days
	0.437905[b]	Aging coefficient based on $t_0 = t_s = 4$ days and $t_f = 10{,}000$ days

Note: material properties of the concrete have been calculated in accordance with (CEB-FIB, 1993).
[a] Calculated to account for creep effects using the AEMM method.
[b] Calculated to account for shrinkage effects using the MS method.

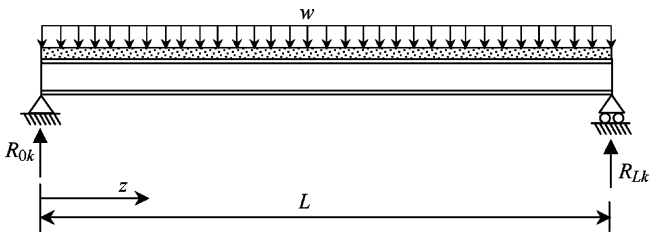

Fig. 5. Composite beam: simply supported beam.

$$v_k = \frac{wz^3}{24}(2L - z)\tilde{\lambda}_{1r} + \frac{r_{3k}}{\mu_k}\tilde{e}_k(z) + \frac{w}{k}\left[\frac{\tilde{\lambda}_{3r}}{\mu_0}\tilde{e}_0(z) + \frac{\tilde{\lambda}_{4r}z^2}{2}\right] + \frac{Sh_{2k}\varepsilon_{sh}z^2}{2} + \widehat{C}_{1k}z + \widehat{C}_{2k} \tag{48}$$

where

$$\widehat{C}_{1k} = -\frac{L}{24k}\left(\tilde{\lambda}_{1r}wL^2k + 12w\tilde{\lambda}_{4r} + 12Sh_{2k}\varepsilon_{sh}k\right) \tag{49}$$

$$\widehat{C}_{2k} = -\frac{r_{3k}\widetilde{Y}_k k\mu_0(1 + e^{-\mu_k L}) + w\widetilde{Y}_0\mu_k\tilde{\lambda}_{3r}(1 + e^{-\mu_0 L})}{\mu_k\mu_0 k} \tag{50}$$

while the strain and the axial displacement at the level of the reference axis are

$$\tilde{\varepsilon}_{bk} = \frac{wz}{2}(L-z)\tilde{\lambda}_{1l} + l_{3k}\mu_k\tilde{e}_k(z) + \frac{w}{k}\left[\mu_0\tilde{\lambda}_{3l}\tilde{e}_0(z) + \tilde{\lambda}_{4l}\right] + Sh_{3k}\varepsilon_{\mathrm{sh}} \tag{51}$$

$$u_{bk} = \frac{wz^2}{12}(3L-2z)\tilde{\lambda}_{1l} + l_{3k}\tilde{\tilde{e}}_k(z) + \frac{w}{k}\left[\tilde{\lambda}_{3l}\tilde{\tilde{e}}_0(z) + \tilde{\lambda}_{4l}z\right] + Sh_{3k}\varepsilon_{\mathrm{sh}}z + C_{uk} \tag{52}$$

where

$$C_{uk} = -\frac{l_{3k}\widetilde{Y}_k k(\mathrm{e}^{-\mu_k L}-1) + w\widetilde{Y}_0\tilde{\lambda}_{3l}(\mathrm{e}^{-\mu_0 L}-1)}{k} \tag{53}$$

The results of the closed form solutions are in exact agreement with those obtained using the direct stiffness approach as shown in Figs. 6 and 7 for the deflection along a simply supported beam 10 m long subjected to a uniformly distributed load of 25 kN/m (i.e. its self-weight) and to shrinkage deformation respectively.

7.3. Encastré composite beam subject to a uniformly distributed load and to shrinkage deformation

Fig. 8 shows a beam encastré at its ends. From the symmetry of its loading and of its support conditions

$$R_{0k} = R_{Lk} = \frac{wL}{2}; \quad M_{0k} = -M_{Lk}; \quad N_{0k} = -N_{Lk} \tag{54a, b, c}$$

where R_{Lk}, N_{Lk} and M_{Lk} are the vertical and horizontal reactions and the moment at the right hand support ($z = L$) calculated at time t.

The shrinkage deformation does not induce any displacements and deformations along the length of the fixed ended beam. It also produces no stresses in the steel joist and in the reinforcing bars, while it produces a stress equal to $-E_{\mathrm{e}}\varepsilon_{\mathrm{sh}}$ in the concrete component. For this reason, the following expressions describe the behaviour of the fixed ended beam subjected to the uniformly distributed load only.

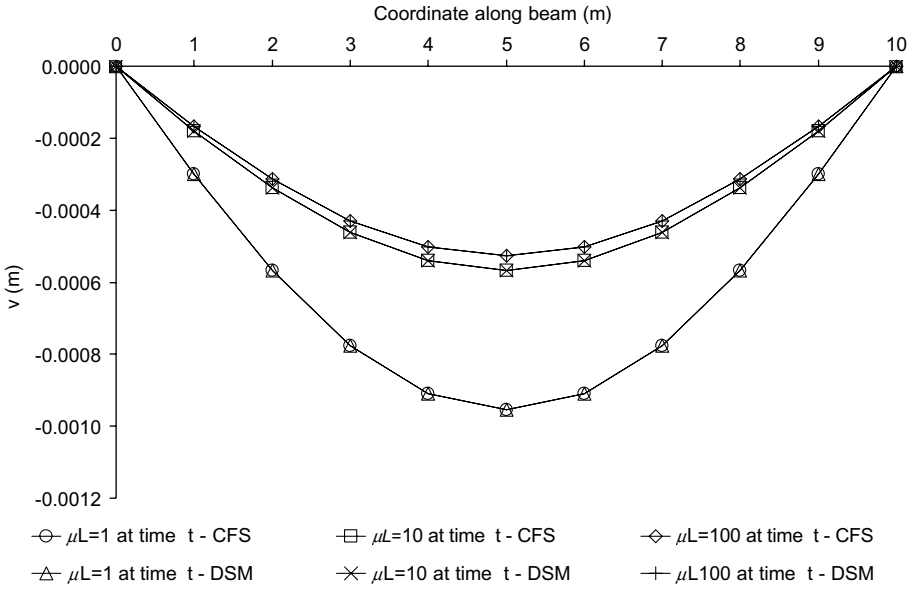

Fig. 6. Variation of the deflection along a simply supported beam subjected to a uniformly distributed load at time $t = 10{,}000$ days for various levels of the dimensionless stiffness coefficient $\mu_k L$ (CFS = closed form solution, DSM = direct stiffness method).

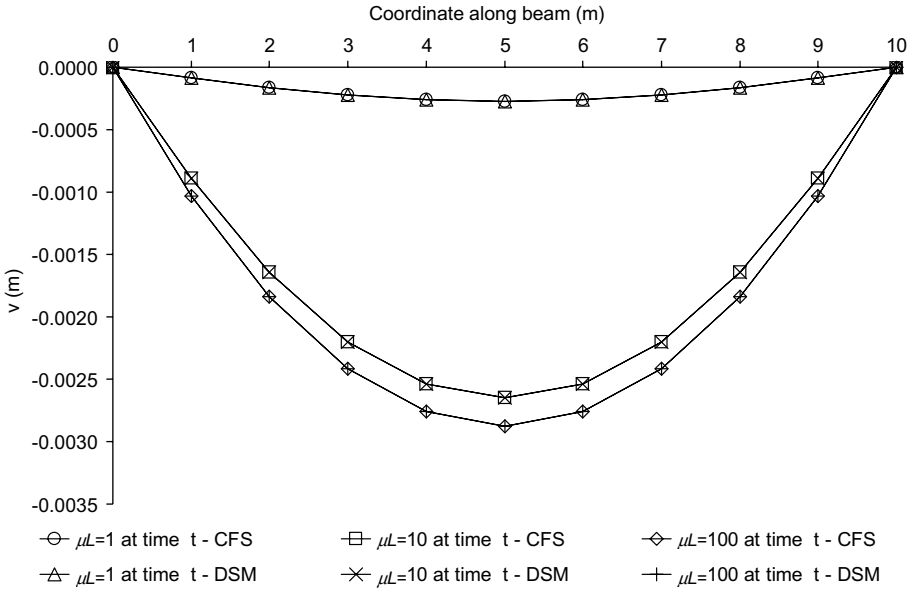

Fig. 7. Variation of the deflection along a simply supported beam subjected to shrinkage effects at time $t = 10{,}000$ days for various levels of the dimensionless stiffness coefficient $\mu_k L$ (CFS = closed form solution, DSM = direct stiffness method).

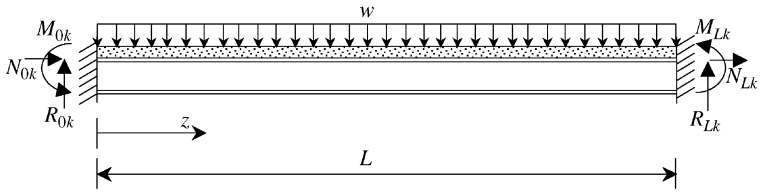

Fig. 8. Composite beam: encastré beam.

Applying the static kinematic conditions that $s_k(z = 0) = 0$ and $s_k(z = L) = 0$, the constants of integration C_{1k} and C_{2k} that are related to the slip and the slip strain can be determined, and the expressions for the slip and slip strain become

$$s_k = \frac{w}{k}\left[L\bar{\bar{e}}_k(z) + L\tilde{\lambda}_2\bar{\bar{e}}_0(z) - \left(\frac{L}{2} - z\right)\tilde{\lambda}_{1\alpha}\right] \tag{55}$$

$$\dot{s}_k = \frac{w}{k}\left[L\mu_k\bar{e}_k(z) + L\mu_0\tilde{\lambda}_2\bar{e}_0(z) + \tilde{\lambda}_{1\alpha}\right] \tag{56}$$

The strain in the top fibre of the cross-section, the curvature, the rotation and the deflection along the beam can be determined as

$$\tilde{\varepsilon}_{0k} = \frac{w}{12}\left(-L^2 + 6Lz - 6z^2\right)\tilde{\lambda}_{1b} + \frac{wL}{k}\left[\mu_k b_{3k}\bar{e}_k(z) + \mu_0\tilde{\lambda}_{3b}\bar{e}_0(z) + \frac{\tilde{\lambda}_{4b}}{L}\right] \tag{57}$$

$$\rho_k = \frac{w}{12}\left(-L^2 + 6Lz - 6z^2\right)\tilde{\lambda}_{1r} + \frac{wL}{k}\left[\mu_k r_{3k}\bar{e}_k(z) + \mu_0\tilde{\lambda}_{3r}\bar{e}_0(z) + \frac{\tilde{\lambda}_{4r}}{L}\right] \tag{58}$$

$$\theta_k = \frac{wz}{12}\left(-L^2 + 3Lz - 2z^2\right)\tilde{\lambda}_{1r} + \frac{wL}{k}\left[r_{3k}\bar{\bar{e}}_k(z) + \tilde{\lambda}_{3r}\bar{\bar{e}}_0(z) + \frac{\tilde{\lambda}_{4r}}{L}z\right] + \widehat{C}_{1k} \tag{59}$$

$$v_k = \frac{wz^2}{24}\left(-L^2 + 2Lz - z^2\right)\tilde{\lambda}_{1r} + \frac{wL}{k}\left[\frac{r_{3k}\bar{e}_k(z)}{\mu_k} + \frac{\tilde{\lambda}_{3r}\bar{e}_0(z)}{\mu_0} + \frac{\tilde{\lambda}_{4r}}{2L}z^2\right] + \widehat{C}_{1k}z + \widehat{C}_{2k} \tag{60}$$

where

$$\widehat{C}_{1k} = -\frac{w}{k}\left[LY_k r_{3k}\left(\mathrm{e}^{-\mu_k L} - 1\right) + LY_0\tilde{\lambda}_{3r}\left(\mathrm{e}^{-\mu_0 L} - 1\right)\right] \tag{61}$$

$$\widehat{C}_{2k} = -\frac{w}{k}\left[\frac{LY_k r_{3k}}{\mu_k}\left(\mathrm{e}^{-\mu_k L} + 1\right) + \frac{LY_0\tilde{\lambda}_{3r}}{\mu_0}\left(\mathrm{e}^{-\mu_0 L} + 1\right)\right] \tag{62}$$

while the strain and the axial displacement at the level of the reference axis are:

$$\tilde{\varepsilon}_{bk} = \frac{w}{12}\left(-L^2 + 6Lz - 6z^2\right)\tilde{\lambda}_{1l} + \frac{wL}{k}\left[\mu_k l_{3k}\bar{e}_k(z) + \mu_0\tilde{\lambda}_{3l}\bar{e}_0(z) + \frac{\tilde{\lambda}_{4l}}{L}\right] \tag{63}$$

$$u_{bk} = \frac{wz}{12}\left(-L^2 + 3Lz - 2z^2\right)\tilde{\lambda}_{1l} + \frac{wL}{k}\left[l_{3k}\bar{\bar{e}}_k(z) + \tilde{\lambda}_{3l}\bar{\bar{e}}_0(z) + \frac{\tilde{\lambda}_{4l}}{L}z\right] + C_{uk} \tag{64}$$

where

$$C_{uk} = -\frac{w}{k}\left[LY_k l_{3k}\left(\mathrm{e}^{-\mu_k L} - 1\right) + LY_0\tilde{\lambda}_{3l}\left(\mathrm{e}^{-\mu_0 L} - 1\right)\right] \tag{65}$$

The values of the moments and of the horizontal reactions at the supports are calculated imposing $\theta_k(z=0) = 0$ and $u_{bk}(z=0) = 0$ respectively, which yield

$$M_{0k} = -M_{Lk} = \frac{wL^2}{12} \tag{66}$$

$$N_{0k} = -N_{Lk} = 0 \tag{67}$$

Eq. (66) implies that the points of contraflexure for a beam encastré at both ends are independent of the value of the shear connection stiffness and are located at the same position as those for a beam with full shear interaction. This was also shown to be the case by Ranzi et al. (2003) for an instantaneous analysis.

The results obtained using the closed form solutions and the direct stiffness method match exactly as shown in Fig. 9 for the deflection along a 14 m encastré beam subjected to 25 kN/m (i.e. its self-weight).

7.4. Propped cantilever subject to a uniformly distributed load and to shrinkage deformation

The left hand end of the propped cantilever ($z = 0$) shown in Fig. 10 is assumed to be fixed while the right hand end ($z = L$) is assumed to be a roller support. From statics, the reactions at time t can be expressed as

$$R_{0k} = wL - R_{Lk}; \quad M_{Lk} = 0 \tag{68a, b}$$

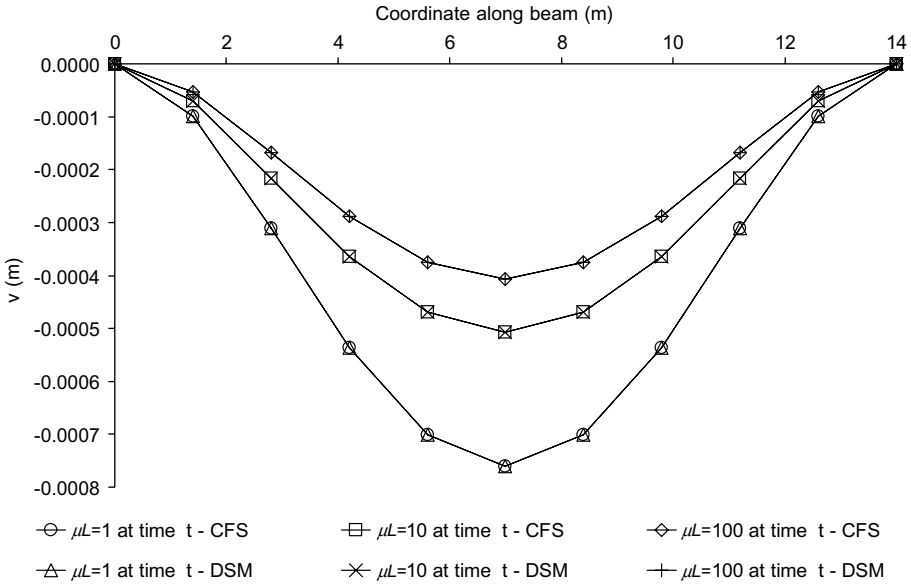

Fig. 9. Variation of the deflection along an encastré beam subjected to a uniformly distributed load at time $t = 10{,}000$ days for various levels of the dimensionless stiffness coefficient $\mu_k L$ (CFS = closed form solution, DSM = direct stiffness method).

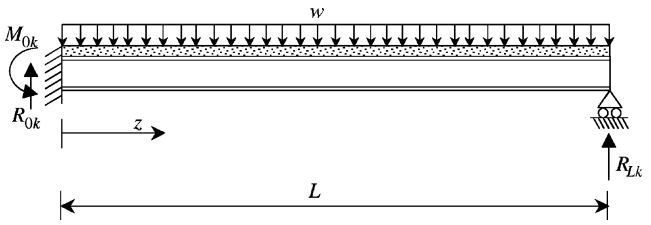

Fig. 10. Composite beam: propped cantilever.

$$M_{0k} = \frac{wL^2}{2} - R_{Lk}L; \quad N_{0k} = N_{Lk} = 0 \tag{68c, d}$$

and so the expressions for the slip and slip strain are defined once the constants of integration $\widetilde{C}_{1k}$ and $\widetilde{C}_{2k}$ are obtained from the kinematic and static boundary conditions that $s_k(z=0) = 0$ and $\dot{s}_k(z=L) = -\tilde{\varepsilon}_{\mathrm{sh}}$. Hence,

$$s_k = \hat{e}_k(z) + \frac{\tilde{\lambda}_{1\alpha} wz - \tilde{\lambda}_{0\alpha}}{k} + \tilde{\lambda}_2 \hat{e}_0(z) \tag{69}$$

$$\dot{s}_k = v_k \hat{\hat{e}}_k(z) + \frac{w\tilde{\lambda}_{1\alpha}}{k} + \mu_0 \hat{\hat{e}}_0(z)\tilde{\lambda}_2 \tag{70}$$

The strain in the top fibre of the composite cross-section, the curvature, the rotation and the deflection along the beam can be determined as follows

$$\tilde{\varepsilon}_{0k} = \frac{w}{2}\left(L^2 - z^2\right)\tilde{\lambda}_{1b} - (L-z)\tilde{\lambda}_{0b} + \frac{w}{k}\tilde{\lambda}_{4b} + b_{3k}\mu_k \hat{\hat{e}}_k(z) + \mu_0 \hat{\hat{e}}_0(z)\tilde{\lambda}_{3b} + Sh_{1k}\varepsilon_{\mathrm{sh}} \tag{71}$$

$$\rho_k = \frac{w}{2}\left(L^2 - z^2\right)\tilde{\lambda}_{1r} - (L - z)\tilde{\lambda}_{0r} + \frac{w}{k}\tilde{\lambda}_{4r} + r_{3k}\mu_k\hat{\tilde{e}}_k(z) + \mu_0\hat{\tilde{e}}_0(z)\tilde{\lambda}_{3r} + Sh_{2k}\varepsilon_{\mathrm{sh}} \tag{72}$$

$$\theta_k = \frac{wz}{6}\left(3L^2 - z^2\right)\tilde{\lambda}_{1r} - \left(Lz - \frac{z^2}{2}\right)\tilde{\lambda}_{0r} + \frac{w}{k}\tilde{\lambda}_{4r}z + r_{3k}\hat{\tilde{e}}_k(z) + \tilde{\lambda}_{3r}\hat{\tilde{e}}_0(z) + Sh_{2k}\varepsilon_{\mathrm{sh}}z + \widehat{C}_{1k} \tag{73}$$

$$v_k = \frac{wz^2}{24}\left(6L^2 - z^2\right)\tilde{\lambda}_{1r} - \frac{z^2}{6}(3L - z)\tilde{\lambda}_{0r} + \frac{w}{2k}\tilde{\lambda}_{4r}z^2 + \frac{r_{3k}}{\mu_k}\hat{\tilde{e}}_k(z) + \frac{\tilde{\lambda}_{3r}}{\mu_0}\hat{\tilde{e}}_0(z) + \frac{Sh_{2k}\varepsilon_{\mathrm{sh}}}{2}z^2 + \widehat{C}_{1k}z + \widehat{C}_{2k} \tag{74}$$

where

$$\widehat{C}_{1k} = \frac{L^2}{3}(-r_{1k}\tilde{\varphi}m_1 - r_{2k}\tilde{\varphi}m_2)\left(\widetilde{R}_{00} - \frac{5wL}{8}\right) + \frac{r_{1k}L^2}{3}\left(R_{0k} - \frac{5wL}{8}\right) - \frac{Sh_{2k}\varepsilon_{\mathrm{sh}}L}{2} - \frac{w\tilde{\lambda}_{4r}L}{2k} + \tilde{\lambda}_5 \tag{75}$$

$$\widehat{C}_{2k} = -r_{3k}\frac{\widetilde{C}_{1k} - \widetilde{C}_{2k}}{\mu_k} - \tilde{\lambda}_{3r}\frac{\widetilde{C}_{10} - \widetilde{C}_{20}}{\mu_0} \tag{76}$$

while the strain and the axial displacement at the level of the reference axis are

$$\tilde{\varepsilon}_{bk} = \frac{w}{2}\left(L^2 - z^2\right)\tilde{\lambda}_{1l} - (L - z)\tilde{\lambda}_{0l} + \frac{w}{k}\tilde{\lambda}_{4l} + l_{3k}\mu_k\hat{\tilde{e}}_k(z) + \mu_0\hat{\tilde{e}}_0(z)\tilde{\lambda}_{3l} + Sh_{3k}\varepsilon_{\mathrm{sh}} \tag{77}$$

$$u_{bk} = \frac{wz}{6}\left(3L^2 - z^2\right)\tilde{\lambda}_{1l} - \left(Lz - \frac{z^2}{2}\right)\tilde{\lambda}_{0l} + \frac{w}{k}\tilde{\lambda}_{4l}z + l_{3k}\hat{\tilde{e}}_k(z) + \tilde{\lambda}_{3l}\hat{\tilde{e}}_0(z) + Sh_{3k}\varepsilon_{\mathrm{sh}}z + C_{uk} \tag{78}$$

and

$$C_{uk} = -l_{3k}\left(\widetilde{C}_{1k} + \widetilde{C}_{2k}\right) - \tilde{\lambda}_{3l}\left(\widetilde{C}_{10} + \widetilde{C}_{20}\right) \tag{79}$$

The value of the reaction at the fixed support ($z = 0$) is calculated using $\theta(z = 0)$ as

$$R_{0k} = \frac{L\mu_k\mu_0 k\tilde{\lambda}_6 + 12w\tilde{\lambda}_{4r}L^2\mu_k\mu_0 + \tilde{\lambda}_7}{8\mu_0 k\left\{L^3\mu_k r_{1k} + 3r_{3k}\widetilde{C}_{s2}\mathrm{e}^{-2\mu_k L}(L\mu_k - \mathrm{e}^{\mu_k L} + 1) + 3r_{3k}\widetilde{C}_{s2}(L\mu_k + \mathrm{e}^{-\mu_k L} - 1)\right\}} \tag{80}$$

As for the previous structural systems, the derived closed form solutions and the direct stiffness method yield identical results; this is shown in Figs. 11 and 12 for the deflection of a 12 m propped cantilever subjected to a uniformly distributed load of 25 kN/m (i.e. its self-weight) and to shrinkage deformation respectively.

8. Conclusions

This paper has proposed a generic modelling for the time-dependent analysis of composite steel–concrete beams with partial shear interaction for which both creep and shrinkage effects have been accounted for. The composite cross-section has been assumed to be formed by a steel joist, a shear connection and a reinforced concrete slab; the steel joist, the reinforcement and the shear connection are assumed to behave in a linear-elastic fashion, while the concrete component is assumed to be time-dependent and its behaviour is modelled using methods (i.e. AEMM and MS methods) that lend themselves to algebraic representation.

The model can be applied to the analysis of continuous beams subjected to generic loading conditions. The application of this model for the time analysis of simply supported beams, encastré beams and propped

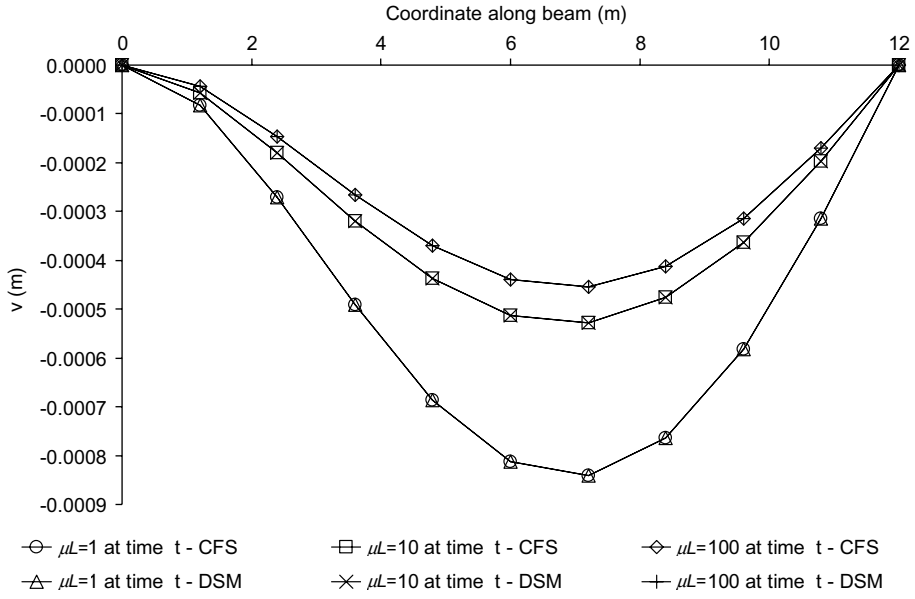

Fig. 11. Variation of the deflection along a propped cantilever beam subjected to a uniformly distributed load at time $t = 10{,}000$ days for various levels of the dimensionless stiffness coefficient $\mu_k L$ (CFS = closed form solution, DSM = direct stiffness method).

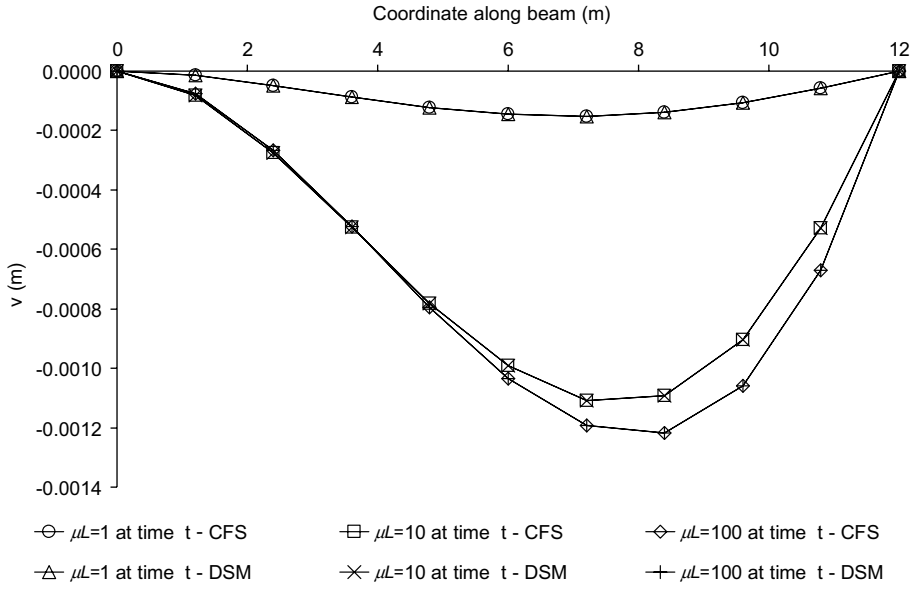

Fig. 12. Variation of the deflection along a propped cantilever beam subjected to shrinkage effects at time $t = 10{,}000$ days for various levels of the dimensionless stiffness coefficient $\mu_k L$ (CFS = closed form solution, DSM = direct stiffness method).

cantilever beams has been illustrated when subjected to uniformly distributed loading and shrinkage deformations. Various representations of the structural behaviour of these beams have been expressed in closed form. The accuracy of the results obtained using these closed form solutions has been validated against

results obtained by means of the direct stiffness method. It was shown that the results obtained using the closed form solutions and the direct stiffness method are in exact agreement. Whilst being too complex for hand calculations, the closed form solutions may be programmed readily so that the influence of the various parameters that affect the behaviour of composite beams can be investigated. These can also be used to benchmark other modelling techniques, i.e. based on the finite element method or finite difference method, which require two discretisations to accomplish a time analysis, i.e. a spatial one along the beam and one in the time domain.

Appendix A

A_c, A_r, A_s = area of the concrete component, of the reinforcement and of the steel joist respectively.

$$A\widetilde{E}_{1\gamma} = A_c\left[E_c + (E_e - E_c)\tilde{\delta}_\gamma\right] + A_r E_r; \quad A\widetilde{E}_{2\gamma} = A_s E_s; \quad A\widetilde{E}_\gamma = A\widetilde{E}_{1\gamma} + A\widetilde{E}_{2\gamma}$$

$$a_{10} = -\tilde{\phi}_{11}M_{00} - \tilde{\phi}_{12}N_{00} + \tilde{\phi}_{13}\frac{w\alpha_0}{k}; \quad a_{20} = \tilde{\phi}_{11}R_{00}; \quad a_{30} = -\tilde{\phi}_{11}\frac{w}{2}; \quad a_{40} = \tilde{\phi}_{13}\mu_0 C_{10}$$

$$a_{50} = -\tilde{\phi}_{13}\mu_0 C_{20}; \quad a_{110} = -\tilde{\phi}_{21}M_{00} - \tilde{\phi}_{22}N_{00} + \tilde{\phi}_{23}\frac{w\alpha_0}{k}; \quad a_{120} = \tilde{\phi}_{21}R_{00}; \quad a_{130} = -\tilde{\phi}_{21}\frac{w}{2}$$

$$a_{140} = \tilde{\phi}_{23}\mu_0 C_{10}; \quad a_{150} = -\tilde{\phi}_{23}\mu_0 C_{20}$$

B_c, B_r, B_s = first moment of area of the concrete component, of the reinforcement and of the steel joist respectively.

$$B\widetilde{E}_{1\gamma} = B_c\left[E_c + (E_e - E_c)\tilde{\delta}_\gamma\right] + B_r E_r; \quad B\widetilde{E}_{2\gamma} = B_s E_s; \quad B\widetilde{E}_\gamma = B\widetilde{E}_{1\gamma} + B\widetilde{E}_{2\gamma}$$

$$b_{1\gamma} = -\frac{B\widetilde{E}_\gamma + y_0 A\widetilde{E}_\gamma}{A\widetilde{E}_\gamma I\widetilde{E}_\gamma - B\widetilde{E}_\gamma^2}; \quad b_{2\gamma} = \frac{y_0 B\widetilde{E}_\gamma + I\widetilde{E}_\gamma}{A\widetilde{E}_\gamma I\widetilde{E}_\gamma - B\widetilde{E}_\gamma^2}$$

$$b_{3\gamma} = \frac{B\widetilde{E}_\gamma B\widetilde{E}_{2\gamma} + y_0\left(B\widetilde{E}_{2\gamma}A\widetilde{E}_{1\gamma} - B\widetilde{E}_{1\gamma}A\widetilde{E}_{2\gamma}\right) - A\widetilde{E}_{2\gamma}I\widetilde{E}_\gamma}{A\widetilde{E}_\gamma I\widetilde{E}_\gamma - B\widetilde{E}_\gamma^2}$$

C_{10}, C_{20} = constants of integration for the slip and slip strain at time t_0

$$\widetilde{C}_{10} = \frac{\alpha_0 e^{-\mu_0 L}}{k\mu_0}\frac{\mu_0\widetilde{R}_{00}e^{-\mu_0 L} - w}{1 + e^{-2\mu_0 L}}; \quad \widetilde{C}_{20} = \frac{\alpha_0}{k\mu_0}\frac{\mu_0\widetilde{R}_{00} + we^{-\mu_0 L}}{1 + e^{-2\mu_0 L}}$$

$$\widetilde{C}_{1k} = \widetilde{C}_{s2}e^{-2\mu_k L}R_{0k} + \widetilde{C}_{s1}e^{-2\mu_k L} - \widetilde{C}_{s3}; \quad \widetilde{C}_{2k} = \widetilde{C}_{s2}R_{0k} + \widetilde{C}_{s1} + \widetilde{C}_{s3}$$

$$\widetilde{C}_{s1} = \frac{-\widetilde{R}_{00}\left(\alpha_0\tilde{\lambda}_2 + \alpha_k\tilde{\varphi}m_1 + \alpha_{2k}\tilde{\varphi}m_2\right)}{k(1 + e^{-2\mu_k L})}; \quad \widetilde{C}_{s2} = \frac{\alpha_k}{k(1 + e^{-2\mu_k L})}; \quad \widetilde{C}_{s3} = \frac{\tilde{\varepsilon}_{sh}e^{-\mu_k L}k - we^{-\mu_k L}\left(\alpha_0\tilde{\lambda}_2 - \tilde{\lambda}_{1\alpha}\right)}{\mu_k k(1 + e^{-2\mu_k L})}$$

E_e, E_c, E_r, E_s = age-adjusted effective modulus, elastic moduli of the concrete component, of the reinforcement and of the steel joist respectively.

$$\tilde{e}_\gamma(z) = \widetilde{Y}_\gamma\left(e^{-\mu_\gamma L}e^{\mu_\gamma z} + e^{-\mu_\gamma z}\right); \quad \tilde{\tilde{e}}_\gamma(z) = \widetilde{Y}_\gamma\left(e^{-\mu_\gamma L}e^{\mu_\gamma z} - e^{-\mu_\gamma z}\right)$$

$$\bar{e}_\gamma(z) = Y_\gamma\left(\mathrm{e}^{-\mu_\gamma L}\mathrm{e}^{\mu_\gamma z} + \mathrm{e}^{-\mu_\gamma z}\right); \quad \bar{\bar{e}}_\gamma(z) = Y_\gamma\left(\mathrm{e}^{-\mu_\gamma L}\mathrm{e}^{\mu_\gamma z} - \mathrm{e}^{-\mu_\gamma z}\right)$$

$$\hat{e}_\gamma(z) = \widetilde{C}_{1\gamma}\mathrm{e}^{\mu_\gamma z} + \widetilde{C}_{2\gamma}\mathrm{e}^{-\mu_\gamma z}; \quad \hat{\hat{e}}_\gamma(z) = \widetilde{C}_{1\gamma}\mathrm{e}^{\mu_\gamma z} - \widetilde{C}_{2\gamma}\mathrm{e}^{-\mu_\gamma z}$$

$$\tilde{f}_{1\gamma}(p,p_{\mathrm{sh}}) = p_{3\gamma}\left(\psi_{2\gamma} + \frac{\alpha_\gamma w}{k}\right) - p_{1\gamma}\delta_{1\gamma} - p_{2\gamma}\delta_{11\gamma} + p_{\mathrm{sh}}\varepsilon_{\mathrm{sh}}; \quad \tilde{f}_{2\gamma}(p,p_{\mathrm{sh}}) = -p_{1\gamma}\delta_{2\gamma} - p_{2\gamma}\delta_{12\gamma}$$

$$\tilde{f}_{3\gamma}(p,p_{\mathrm{sh}}) = -p_{1\gamma}\frac{w}{2} - p_{1\gamma}\delta_{3\gamma} - p_{2\gamma}\delta_{13\gamma}; \quad \tilde{f}_{4\gamma}(p,p_{\mathrm{sh}}) = p_{3\gamma}\mu_0\psi_{3\gamma} - p_{1\gamma}\delta_{4\gamma} - p_{2\gamma}\delta_{14\gamma}$$

$$\tilde{f}_{5\gamma}(p,p_{\mathrm{sh}}) = -p_{3\gamma}\mu_0\psi_{4\gamma} - p_{1\gamma}\delta_{5\gamma} - p_{2\gamma}\delta_{15\gamma}$$

I_{c}, I_{r}, I_{s} = second moment of area of the concrete component, of the reinforcement and of the steel joist respectively.

$$I\widetilde{E}_{1\gamma} = I_{\mathrm{c}}\left[E_{\mathrm{c}} + (E_{\mathrm{e}} - E_{\mathrm{c}})\tilde{\delta}_\gamma\right] + I_{\mathrm{r}}E_{\mathrm{r}}; \quad I\widetilde{E}_{2\gamma} = I_{\mathrm{s}}E_{\mathrm{s}}; \quad I\widetilde{E}_\gamma = I\widetilde{E}_{1\gamma} + I\widetilde{E}_{2\gamma}$$

$$l_{1\gamma} = b_{1\gamma} + y_0 r_{1\gamma}; \quad l_{2\gamma} = b_{2\gamma} + y_0 r_{2\gamma}; \quad l_{3\gamma} = b_{3\gamma} + y_0 r_{3\gamma} + 1; \quad Sh_{3k} = Sk_{1k} + y_0 Sh_{2k}$$

M_{00} = moment at the left end of the beam at time t_0

$$m_1 = \phi_{\mathrm{c}10}b_{10} + \phi_{\mathrm{c}20}r_{10}; \quad m_2 = \phi_{\mathrm{c}30}b_{10} + \phi_{\mathrm{c}40}r_{10}$$

N_{00} = horizontal reaction at the left end of the beam at time t_0

$$n_1 = \phi_{\mathrm{c}10}b_{30} + \phi_{\mathrm{c}20}r_{30}; \quad n_2 = \phi_{\mathrm{c}30}b_{30} + \phi_{\mathrm{c}40}r_{30}$$

$$q_{10} = \frac{B\widetilde{E}_{10}A\widetilde{E}_{20} - B\widetilde{E}_{20}A\widetilde{E}_{10}}{A\widetilde{E}_0 I\widetilde{E}_0 - B\widetilde{E}_0^2}; \quad q_{20} = \frac{A\widetilde{E}_{10}I\widetilde{E}_0 - B\widetilde{E}_{10}B\widetilde{E}_0}{A\widetilde{E}_0 I\widetilde{E}_0 - B\widetilde{E}_0^2}$$

$$q_{30} = \frac{B\widetilde{E}_{10}^2 A\widetilde{E}_{20} + B\widetilde{E}_{20}^2 A\widetilde{E}_{10} - I\widetilde{E}_0 A\widetilde{E}_{10}A\widetilde{E}_{20}}{A\widetilde{E}_0 I\widetilde{E}_0 - B\widetilde{E}_0^2}$$

$$q_{1k} = \frac{B\widetilde{E}_{1k}A\widetilde{E}_{2k} - B\widetilde{E}_{2k}A\widetilde{E}_{1k}}{A\widetilde{E}_k I\widetilde{E}_k - B\widetilde{E}_k^2}; \quad q_{2k} = \frac{A\widetilde{E}_{1k}I\widetilde{E}_k - B\widetilde{E}_{1k}B\widetilde{E}_k}{A\widetilde{E}_k I\widetilde{E}_k - B\widetilde{E}_k^2}$$

$$q_{3k} = \frac{B\widetilde{E}_{1k}^2 A\widetilde{E}_{2k} + B\widetilde{E}_{2k}^2 A\widetilde{E}_{1k} - I\widetilde{E}_k A\widetilde{E}_{1k}A\widetilde{E}_{2k}}{A\widetilde{E}_k I\widetilde{E}_k - B\widetilde{E}_k^2}; \quad q_{4k} = -\frac{A\widetilde{E}_{2k}I\widetilde{E}_k - B\widetilde{E}_{2k}B\widetilde{E}_k}{A\widetilde{E}_k I\widetilde{E}_k - B\widetilde{E}_k^2}$$

R_{00} = vertical reaction at the left end of the beam at time t_0

$$\widetilde{R}_{00} = \frac{5wL}{8}\left\{\frac{(\mathrm{e}^{-2\mu_0 L}+1)\left[5\mu_0^2L^2 + 12\tilde{\mu}_0(\mu_0^2L^2-2)\right] + 48\tilde{\mu}_0\mathrm{e}^{-\mu_0 L}}{5\mu_0 L[(3\tilde{\mu}_0+1)(1+\mathrm{e}^{-2\mu_0 L})\mu_0 L + 3\tilde{\mu}_0(\mathrm{e}^{-2\mu_0 L}-1)]}\right\}$$

$$r_{1\gamma} = \frac{A\widetilde{E}_\gamma}{A\widetilde{E}_\gamma I\widetilde{E}_\gamma - B\widetilde{E}_\gamma^2}; \quad r_{2\gamma} = \frac{-B\widetilde{E}_\gamma}{A\widetilde{E}_\gamma I\widetilde{E}_\gamma - B\widetilde{E}_\gamma^2}; \quad r_{3\gamma} = \alpha_\gamma$$

$$Sh_{1k} = \frac{\left(I\widetilde{E}_k + y_0 B\widetilde{E}_k\right)A_c E_e - \left(B\widetilde{E}_k + y_0 A\widetilde{E}_k\right)B_c E_e}{A\widetilde{E}_k I\widetilde{E}_k - B\widetilde{E}_k^2}; \quad Sh_{2k} = \frac{A\widetilde{E}_k B_c E_e - B\widetilde{E}_k A_c E_e}{A\widetilde{E}_k I\widetilde{E}_k - B\widetilde{E}_k^2}$$

$$Sh_{3k} = Sk_{1k} + y_0 Sh_{2k}; \quad Sh_{4k} = \frac{B\widetilde{E}_k B\widetilde{E}_{2k} - I\widetilde{E}_k A\widetilde{E}_{2k}}{A\widetilde{E}_k I\widetilde{E}_k - B\widetilde{E}_k^2}A_c E_e + \frac{B\widetilde{E}_{1k} A\widetilde{E}_{2k} - A\widetilde{E}_{1k} B\widetilde{E}_{2k}}{A\widetilde{E}_k I\widetilde{E}_k - B\widetilde{E}_k^2}B_c E_e$$

$$Y_0 = \frac{1}{2}\frac{\alpha_0}{e^{-\mu_0 L} - 1}; \quad \widetilde{Y}_0 = -\frac{\alpha_0}{\mu_0(e^{-\mu_0 L} + 1)}; \quad Y_k = \frac{1}{2}\frac{\tilde{\lambda}_{1\alpha} - \alpha_0\tilde{\lambda}_2}{e^{-\mu_k L} - 1}; \quad \widetilde{Y}_k = -\frac{w\tilde{\lambda}_{1\alpha} - w\alpha_0\tilde{\lambda}_2 + \tilde{\varepsilon}_{sh}k}{\mu_k k(e^{-\mu_k L} + 1)}$$

$$\tilde{\alpha}_\gamma = -\frac{B\widetilde{E}_{1\gamma}^2 A\widetilde{E}_{2\gamma} + B\widetilde{E}_{2\gamma}^2 A\widetilde{E}_{1\gamma} - I\widetilde{E}_\gamma A\widetilde{E}_{1\gamma} A\widetilde{E}_{2\gamma}}{A\widetilde{E}_\gamma I\widetilde{E}_\gamma - B\widetilde{E}_\gamma^2}; \quad \alpha_\gamma = \frac{B\widetilde{E}_{1\gamma} A\widetilde{E}_{2\gamma} - B\widetilde{E}_{2\gamma} A\widetilde{E}_{1\gamma}}{A\widetilde{E}_\gamma I\widetilde{E}_\gamma - B\widetilde{E}_\gamma^2}$$

$$\alpha_{1\gamma} = \frac{A\widetilde{E}_{1\gamma} I\widetilde{E}_\gamma - B\widetilde{E}_{1\gamma} B\widetilde{E}_\gamma}{A\widetilde{E}_\gamma I\widetilde{E}_\gamma - B\widetilde{E}_\gamma^2}; \quad \alpha_{2k} = -\frac{A\widetilde{E}_{2k} I\widetilde{E}_k - B\widetilde{E}_{2k} B\widetilde{E}_k}{A\widetilde{E}_k I\widetilde{E}_k - B\widetilde{E}_k^2}$$

$$\beta_{i\gamma} = \tilde{f}_{i\gamma}(b, Sh_{1k}) \text{ with } i = 1, \ldots, 5$$

$\gamma = 0$, k at time t_0 and at time t respectively.

$$\delta_{i\gamma} = \tilde{\varphi} a_{i0}\tilde{\delta}_\gamma \text{ (with } i = 1, \ldots, 5 \text{ and } i = 11, \ldots, 15); \quad \tilde{\delta}_0 = 0; \quad \tilde{\delta}_k = 1$$

$$\tilde{\varepsilon}_{sh} = \frac{A_c E_e}{A\widetilde{E}_{1k}}\varepsilon_{sh}$$

$$\eta_{i\gamma} = \tilde{f}_{i\gamma}(l, Sh_{3k}) \text{ with } i = 1, \ldots, 5$$

$$\tilde{\lambda}_{0\alpha} = \alpha_k R_{0k} - (\alpha_k\tilde{\varphi}m_1 + \alpha_{2k}\tilde{\varphi}m_2)\widetilde{R}_{00}; \quad \tilde{\lambda}_{0x} = x_{1k}R_{0k} - (x_{1k}\tilde{\varphi}m_1 + x_{2k}\tilde{\varphi}m_2)\widetilde{R}_{00}$$

$$\tilde{\lambda}_{1\alpha} = \alpha_k - \alpha_k\tilde{\varphi}m_1 - \alpha_{2k}\tilde{\varphi}m_2; \quad \tilde{\lambda}_{1x} = x_{1k} - x_{1k}\tilde{\varphi}m_1 - x_{2k}\tilde{\varphi}m_2$$

$$\tilde{\lambda}_2 = -\mu_0^2\frac{\alpha_k\tilde{\varphi}n_1 + \alpha_{2k}\tilde{\varphi}n_2}{\tilde{\alpha}_k\mu_0^2 - k}; \quad \tilde{\lambda}_{3x} = x_{3k}\tilde{\lambda}_2 - x_{1k}\tilde{\varphi}n_1 - x_{2k}\tilde{\varphi}n_2$$

$$\tilde{\lambda}_{4x} = x_{3k}\tilde{\lambda}_{1\alpha} - \alpha_0\tilde{\varphi}(x_{1k}n_1 + x_{2k}n_2) \text{ where } x_{ik} \text{ (with } i = 1, 2, 3) \text{ represents a generic variable}$$

$$\tilde{\lambda}_5 = -r_{3k}\frac{\widetilde{C}_{1k}(e^{\mu_k L} - 1) - \widetilde{C}_{2k}(e^{-\mu_k L} - 1)}{L\mu_k} - \tilde{\lambda}_{3r}\frac{\widetilde{C}_{10}(e^{\mu_0 L} - 1) - \widetilde{C}_{20}(e^{-\mu_0 L} - 1)}{L\mu_0}$$

$$\tilde{\lambda}_6 = 12Sh_{2k}\varepsilon_{sh}L + 5wL^3 r_{1k} - L^2(r_{1k}\tilde{\varphi}m_1 + r_{2k}\tilde{\varphi}m_2)\left(5wL - 8\widetilde{R}_{00}\right) - 24\tilde{\lambda}_{3r}\left(\widetilde{C}_{10} + \widetilde{C}_{20}\right) - 24r_{3k}\widetilde{C}_{s1}\left(1 + e^{-2\mu_k L}\right)$$

$$\tilde{\lambda}_7 = 24\tilde{\lambda}_{3r}k\mu_k\left[\widetilde{C}_{10}\left(e^{\mu_0 L} - 1\right) - \widetilde{C}_{20}\left(e^{-\mu_0 L} - 1\right)\right] + 24r_{3k}k\mu_0\left[\left(\widetilde{C}_{s1}e^{-2\mu_k L} - \widetilde{C}_{s3}\right)\left(e^{\mu_k L} - 1\right) - \left(\widetilde{C}_{s1} + \widetilde{C}_{s3}\right)\left(e^{-\mu_k L} - 1\right)\right]$$

$$\mu_\gamma^2 = \frac{k}{\tilde{\alpha}_\gamma}; \quad \tilde{\mu}_0 = \frac{r_{30}\alpha_0}{r_{10}kL^2} = \frac{\left(B\widetilde{E}_{10}A\widetilde{E}_{20} - B\widetilde{E}_{20}A\widetilde{E}_{10}\right)^2}{A\widetilde{E}_0\left(A\widetilde{E}_0 I\widetilde{E}_0 - B\widetilde{E}_0^2\right)kL^2}$$

$$\xi_{i\gamma} = \tilde{f}_{i\gamma}(r, Sh_{2k}) \quad \text{with } i = 1, \ldots, 5$$

$$\phi_{c10} = B_c E_c; \quad \phi_{c20} = (I_c + y_0 B_c)E_c; \quad \phi_{c30} = A_c E_c; \quad \phi_{c40} = (B_c + y_0 A_c)E_c$$

$$\tilde{\phi}_{1i} = \phi_{c10} b_{i0} + \phi_{c20} r_{i0}; \quad \tilde{\phi}_{2i} = \phi_{c30} b_{i0} + \phi_{c40} r_{i0}$$

$$\psi_{1\gamma} = \frac{\alpha_k \delta_{2k} + \alpha_{2k}\delta_{12k}}{k}\tilde{\delta}_\gamma; \quad \psi_{2\gamma} = 2\frac{\alpha_k \delta_{3k} + \alpha_{2k}\delta_{13k}}{k}\tilde{\delta}_\gamma$$

$$\psi_{3\gamma} = \frac{-\alpha_k \mu_0 \delta_{4k} - \alpha_{2k}\mu_0\delta_{14k}}{\tilde{\alpha}_k\mu_0^2 - k}\tilde{\delta}_\gamma; \quad \psi_{4\gamma} = \frac{\alpha_k \mu_0 \delta_{5k} + \alpha_{2k}\mu_0\delta_{15k}}{\tilde{\alpha}_k\mu_0^2 - k}\tilde{\delta}_\gamma$$

References

Amadio, C., Fragiacomo, M., 1993. A finite element model for the study of creep and shrinkage effects in composite beams with deformable shear connections. Costruzioni Metalliche (4), 213–228.

Bažant, Z.P., 1972. Prediction of concrete creep effects using age-adjusted effective modulus method. ACI Journal 69 (4), 212–217.

Bažant, Z.P., Oh, B.H., 1984. Deformation of progressively cracking reinforced concrete beams. ACI Journal 81 (3), 268–278.

Bradford, M.A., Gilbert, R.I., 1989. Nonlinear behaviour of composite beams at service loads. The Structural Engineer 67 (14), 263–268.

Bradford, M.A., Gilbert, R.I., 1992. Composite beams with partial interaction under sustained loads. Journal of Structural Engineering ASCE 118 (7), 1871–1883.

CEB (Comité Euro-International du Béton), 1984. In: Chiorino, M.A., Napoli, P., Mola, F., Koprna, M., (Eds.), CEB Design manual on structural effects of time-dependent behaviour of concrete. Georgi Publishing, Saint-Saphorin, Switzerland.

CEB-FIB (Comité Euro-International du Béton–Fédération International de la Précontrainte), 1993. Model Code 1990: Design Code. Thomas Telford, London, UK.

Dezi, L., Leoni, G., Tarantino, A.M., 1996. Algebraic methods for creep analysis of continuous composite beams. Journal of Structural Engineering ASCE 122 (4), 423–430.

Dezi, L., Leoni, G., Tarantino, A.M., 1998. Creep and shrinkage analysis of composite beams. Progress in Structural Engineering and Materials 1 (2), 170–177.

Dezi, L., Gara, F., Leoni, G., Tarantino, A.M., 2001. Time dependent analysis of shear-lag effect in composite beams. Journal of Engineering Mechanics 127 (1), 71–79.

Fragiacomo, M., Amadio, C., Macorini, L., 2002. Influence of viscous phenomena on steel–concrete composite beams with normal or high performance slab. Steel and Composite Structures 2 (2), 85–98.

Ghali, A., Favre, R., 1994. Concrete Structures: Stresses and Deformations, second ed. E&FN Spon, London.

Gilbert, R.I., 1988. Time Effects in Concrete Structures. Elsevier Science Publishers, Amsterdam, The Netherlands.

Girhammar, U.A., Pan, D., 1993. Dynamic analysis of composite members with interlayer slip. International Journal of Solids and Structures 30 (6), 797–823.

Kwak, H.G., Seo, Y.L., 2002. Time-dependent behaviour of composite beams with flexible connectors. Computer Methods in Applied Mechanics and Engineering 191, 3751–3772.

Newmark, N.M., Siess, C.P., Viest, I.M., 1951. Tests and analysis of composite beams with incomplete interaction. Proceedings of the Society of Experimental Stress Analysis 9 (1), 75–92.

Ranzi, G., 2003. Partial interaction analysis of composite beams using the direct stiffness method. PhD Thesis, The University of New South Wales, Sydney, Australia.

Ranzi, G., Bradford, M.A., Uy, B., 2003. A general method of analysis of composite beams with partial interaction. Steel and Composite Structures 3 (3), 169–184.

Ranzi, G., Bradford, M.A., Gara, F., Leoni, G., 2004a. Partial interaction analysis of composite beams by means of the finite difference method, the finite element method, the direct stiffness method and the analytical solution: a comparative study. In: Proceedings of the 7th International Conference on Computational Structures Technology, Lisbon (Portugal).

Ranzi, G., Bradford, M.A., Uy, B., 2004b. A direct stiffness analysis of a composite beam with partial interaction. International Journal for Numerical Methods in Engineering 61, 657–672.

Tarantino, A.M., Dezi, L., 1992. Creep effects in composite beams with flexible shear connectors. Journal of Structural Engineering ASCE 118 (8), 2063–2081.

Trost, H., 1967. The implications of the principle of superposition for creep and relaxation problems of concrete and prestressed concrete. Beton- und Stahlbetonbau 10, 230–238 (in German).